Wu et al. Nanoscale Research Letters (2017) 12:282
DOI 10.1186/s11671-017-2016-x

Nanoscale Research Letters

NANO EXPRESS Open Access

Direct Growth of Al_2O_3 on Black Phosphorus by Plasma-Enhanced Atomic Layer Deposition

B. B. Wu[1,2], H. M. Zheng[2], Y. Q. Ding[1*], W. J. Liu[2*], H. L. Lu[2], P. Zhou[2], L. Chen[2], Q. Q. Sun[2], S. J. Ding[2] and David W. Zhang[2]

Abstract

Growing high-quality and uniform dielectric on black phosphorus is challenging since it is easy to react with O_2 or H_2O in ambient. In this work, we have directly grown Al_2O_3 on BP using plasma-enhanced atomic layer deposition (PEALD). The surface roughness of BP with covered Al_2O_3 film can reduce significantly, which is due to the removal of oxidized bubble in BP surface by oxygen plasma. It was also found there is an interfacial layer of PO_x in between amorphous Al_2O_3 film and crystallized BP, which is verified by both X-ray photoelectron spectroscopy (XPS) and transmission electron microscopy (TEM) measurements. By increasing temperature, the PO_x can be converted into fully oxidized P_2O_5.

Keywords: Black phosphorus, Plasma-enhanced atomic layer deposition, Oxygen plasma, Al_2O_3

Background

Two-dimensional (2D) semiconductor materials, such as graphene [1, 2], MoS_2 [3, 4], WSe_2 [5], WS_2 [6], $MoTe_2$ [7, 8], $SnSe_2$ [9], and black phosphorous (BP) [10–18], have been widely studied for the potential applications in the next generation devices including field emitters [10–12], gas sensors [13, 14], solar cells [17], field-effect transistors [18], optoelectronics [19], and light-emitting diodes [20]. Among these 2D materials, BP is found to be more thermodynamically stable under the ambient conditions [14]. BP is an anisotropic lamellar semiconductor and has a direct band gap of ~0.3–1.5 eV from the bulk to monolayer structure [21–25]. BP transistors also have high carrier mobility up to 1000 $cm^2/(V \cdot s)$ at room temperature, on/off current ratio over 10^4 [18, 26]. Thus, BP may be a promising candidate for electronic and optoelectronic device applications [27]. However, exfoliated BP films will degrade in the air ambient owing to the possible reactions between BP and the adsorbed water and oxygen, thus leading to a significant reduction of BP carrier mobility and on/off current ratio [27, 28]. Therefore, efficient and reliable isolation/passivation layers are necessary for BP to preserve its inherent structure and property.

So far, many efforts on passivation for BP have been made, such as an encapsulation layer for BP with boron nitride (*h*-BN) [29–33], creating saturated P_2O_5 on BP surface [34–36], atomic layer deposited dielectric capping [27, 37–40]. Nevertheless, *h*-BN passivation requires complicated environmental conditions and has extremely low yield [29–33]. The P_2O_5 which was created on BP surface provides only the short-time protection since the oxygen and moisture in the air can erode it slowly [34–36]. It is also quite tough for atomic layer deposition (ALD) to form a high-quality and uniform top dielectric film on BP because of no dangling bonds. Therefore, it is important to prevent BP-based devices from degradation in the air ambient by covering a protective oxide dielectric. Moreover, uniform and reliable dielectrics are also essentially needed for the top-gate BP devices.

In this work, uniform Al_2O_3 was directly grown on BP flakes using plasma-enhanced atomic layer deposition (PEALD) with the help of O_2 plasma as an oxygen

* Correspondence: yding@jiangnan.edu.cn; wjliu@fudan.edu.cn
[1]The Key Laboratory of Food Colloids and Biotechnology, Ministry of Education, School of Chemical and Material Engineering, Jiangnan University, Wuxi 214122, Jiangsu, China
[2]State Key Lab ASIC & Syst., Department Microelectronics, Fudan University, Shanghai 201203, China

Springer Open

© The Author(s). 2017 **Open Access** This article is distributed under the terms of the Creative Commons Attribution 4.0 International License (http://creativecommons.org/licenses/by/4.0/), which permits unrestricted use, distribution, and reproduction in any medium, provided you give appropriate credit to the original author(s) and the source, provide a link to the Creative Commons license, and indicate if changes were made.

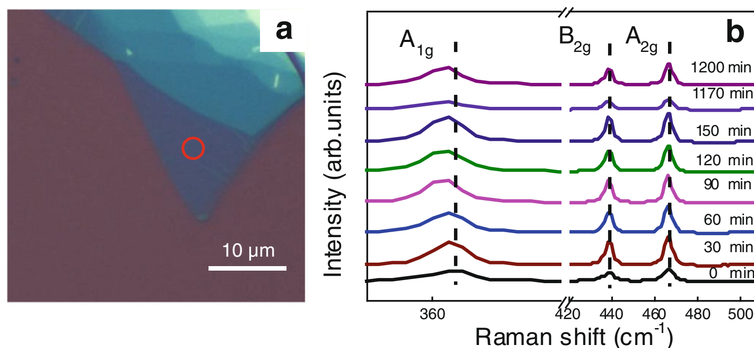

Fig. 1 **a** Optical microscope image of the BP sample acquired by Raman measurements. **b** Raman spectra of pristine BP for different exposure time. All Raman measurements were done in the air ambient with the same laser excitation

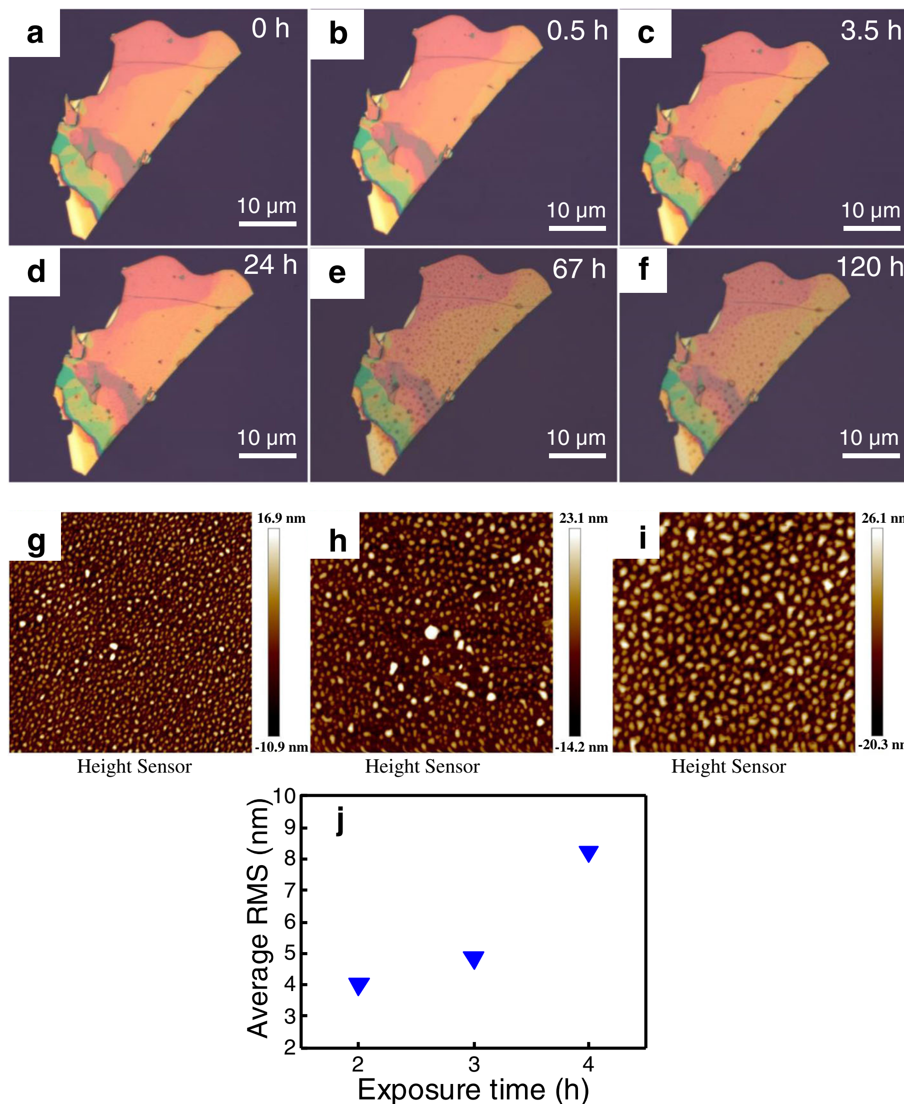

Fig. 2 **a-f** Optical images of accelerated BP degradation on SiO_2/Si exposed to air for different time. **g-i** AFM images of BP flake exposed to the air ambient for 2, 3, and 4 h. All three BP samples for AFM measurements were taken from the same batch. The average thickness of BP in **g–i** was 130 nm. **j** The average RMS roughness of BP samples versus the exposure time, the same samples as shown in **g–i**

precursor, instead of H_2O, to react with trimethylaluminum (TMA) [41]. The composition and properties of the interfacial layer between Al_2O_3 and BP have been examined by physical characterizations, and the mechanisms behind are analyzed.

Methods

Few-layer BP (purity: 99.998%, Smart Elements) was transferred onto a Si substrate with thermally grown 285 nm SiO_2 using a micromechanical method with polydimethylsiloxane (PDMS) [1, 28, 42]. Prior to transfer, the SiO_2 surface was ultrasonically cleaned in turn by acetone and isopropyl alcohol (IPA) and piranha solutions for 10 min each, followed by 100% O_2 annealing at 500 °C for 3 min using rapid thermal annealing (Annealsys As-One). The optical images of BP were acquired by an optical microscope (BA310Met, Motic) equipped with a camera. Raman spectroscopy measurements were performed using LabRam-1B (the Raman spectral resolution was 1.1 cm^{-1}) with an excitation wavelength of 532 nm at room temperature in the air ambient. The laser power was maintained at around 0.5 mW to prevent any heating-induced damage during the measurement. Al_2O_3 films on BP were deposited using PEALD with O_2 plasma and TMA precursors at different temperatures. The freshly exfoliated BP samples were transfer to Picosun 200R ALD chamber (the vacuum pressure was 12 hPa). PEALD of Al_2O_3 was carried out with successive cycles of O_2 plasma and TMA precursors, with an Ar carrier gas (99.9997%, Airgas) at a flow rate of 300 sccm, 15 s pulse + 10 s Ar purge time for O_2 plasma (The O_2 plasma RF Power was 2000 W), 0.1 s pulse + 5 s Ar purge time for TMA (the precursor temperature was 18 °C) at a substrate temperature of 200 °C. The surface and interfacial properties of Al_2O_3 on BP were physically characterized using atomic force microscopy (AFM, Dimension Edge, Bruker), XPS (AXIS ULDLDTRA, Shimadzu), and TEM (Tecnai G^2 F20 S-TWIN, FEI) measurements at room temperature.

Results and Discussion

Figure 1a shows the optical image of transferred BP sample prepared by mechanical exfoliation from its bulky crystalline. The Raman spectra of thin-layer BP, as denoted by a red circle in Fig. 1a, were examined as a function of exposure time in the air ambient at room temperature, as shown in Fig. 1b. It is noted that all Raman spectra measured in Fig. 1b are calibrated using a Si peak of 520 cm^{-1}. It can be clearly seen one out-of-plane modes (A_{1g}) and two in-plane modes (A_{2g} and B_{2g}) in thin-layer BP [43]. Both A_{2g} and B_{2g} peak positions keep almost unchanged. While for A_{1g} mode, it has redshifted as the exposure time goes up to 30 min and then seems to be stable up to 20 h. This may be attributed to the oxidation of surficial BP in the initial stage and a relatively saturation of oxidation up to 20 h. This is evidenced by the time evolution of BP surface morphology examined by optical microscopy, as shown in Fig. 2a–f. It was markedly observed that BP flake exposed to the air ambient degrades as the exposure time extended and then exhibited a fare rough BP surface with bubbles, as presented in Fig. 2d–f. Figure 2g–i shows AFM images of exfoliated BP flake exposed to the air ambient for 2, 3, and 4 h, respectively. All three BP samples for AFM measurements were taken from the same batch and their RMS roughness is summarized in Fig. 2j. The RMS roughness of BP surface increases as the exposure time increases, indicating the formation of oxidative phosphorus species.

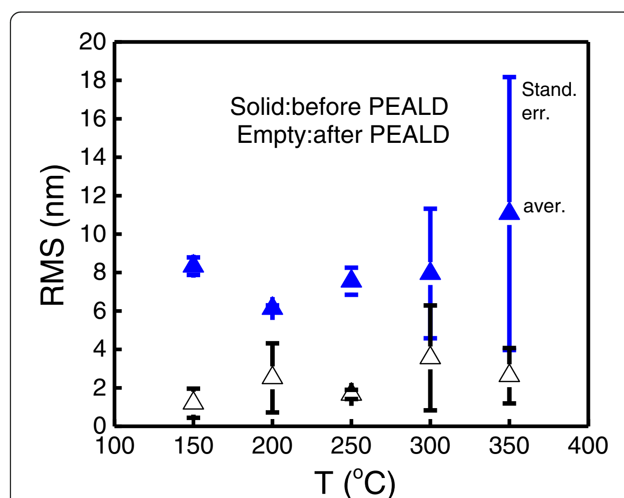

Fig. 3 RMS roughness of BP samples before and after PEALD deposition at various temperatures. For each deposition temperature, more than five samples were measured for an accurate assessment

To evaluate the surface quality of Al_2O_3 film on thin-layer BP, its roughness of RMS was compared quantitatively at different deposition temperatures, as shown in Fig. 3. The corresponding data were summarized in Table 1. Note that more than five samples were measured for each temperature. It was observed that prior to PEALD, the average RMS of thin BP surface is larger than 6 nm, large scattering is due to sample-to-sample

Table 1 The RMS roughness of BP samples before and after PEALD at different temperatures

Temperature (°C)	The average roughness (before/after) (nm)	Standard deviation (before/after) (nm)
150	8.33/1.20	0.46/0.76
200	6.13/2.52	0.16/1.80
250	7.55/1.66	0.71/0.24
300	7.95/3.56	3.34/2.73
350	11.05/2.63	7.10/1.44

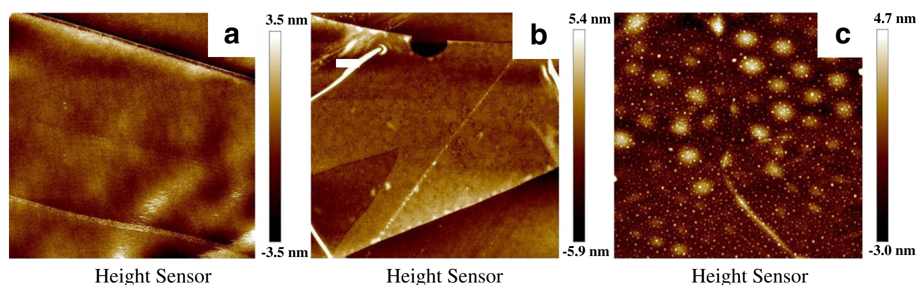

Fig. 4 AFM images of Al_2O_3/BP samples with different deposition recipes at 200 °C. **a** 100 cycles Al_2O_3 on BP grown by PEALD with the pretreatment of 20 cycles O_2 plasma. **b** 100 cycles Al_2O_3 on BP grown by PEALD without any pretreatment. **c** 100 cycles Al_2O_3 on BP grown by ALD with H_2O as an oxygen precursor

variations; however, the RMS reduces to ~3 nm after 100 cycles Al_2O_3 deposition. This infers that O_2 plama as an oxygen precursor can effectively etch the oxidized bubbles in the top-layer BP thin film, thus leading to a significant reduction of RMS, while H_2O as an O source may not have this benefit (discuss later).

To understand the impact of the pretreatment of O_2 plasma and different oxygen precursors on Al_2O_3 growth in freshly exfoliated BP samples, Al_2O_3 deposition on BP was realized by three approaches: (1) 20 cycles O_2 plasma pretrement + 100 cycles TMA/O_2 plasma, (2) 100 cycles TMA/O_2 plasma, and (3) 100 -cycles TMA/H_2O, as shown in Fig. 4a, b, and c, respectively. Figure 4a, b depicts AFM images of the 100 cycles Al_2O_3 grown on BP samples by PEALD with and without an oxygen plasma pretreatment, respectively. Using PEALD for Al_2O_3 growth in BP flakes, it has demonstrated a highly uniform surface morphology of Al_2O_3/BP. The average RMS roughness of Al_2O_3/BP samples prepared by PEALD is only 0.4 nm regardless of an oxygen plasma pretreatment, as shown in Fig. 4a, b. For freshly exfoliated BP samples, PEALD (with and w/o pretreatment) can achieve a good uniformity and coverage of Al_2O_3 films. While for BP samples exposed to the air ambient for certain time, 4 h for example, PEALD with O_2 plasma pretreatment is much preferred. O_2 plasma pretreatment can create enough nucleation sites for ALD growth. On the other hand, it also has an “etching” effect for thinning BP samples. O_2 plasma may penetrate the PO_x layer and oxidize the underlying BP, then increase the thickness of PO_x layer [35]. On the contrary, Al_2O_3 films on freshly exfoliated BP grown by ALD with H_2O as an oxygen precursor nucleate to an isolated “island” and exhibit a remarkable nonuniform surface profile, resulting in a large RMS roughness of 0.8 nm, as shown in Fig. 4c. It is attributed to the insufficient dangling bonds or nucleation sites in BP surface for ALD growth with H_2O as an oxygen precursor [37]. It is worthwhile to mention that BP flake was covered uniformly by Al_2O_3 film and can prevent O_2 or H_2O in air ambient further reacting with BP, thus protected BP from degradation. Otherwise, the uncovered portions of BP surface may react with H_2O and O_2 to produce many bubbles, as shown in Fig. 4c.

Next, chemical analysis of the interfacial characteristics near BP film was examined by XPS characterizations. Figure 5 shows photoelectron spectroscopy measurements of the P 2p core level at different deposition temperatures. Middle and top panels present

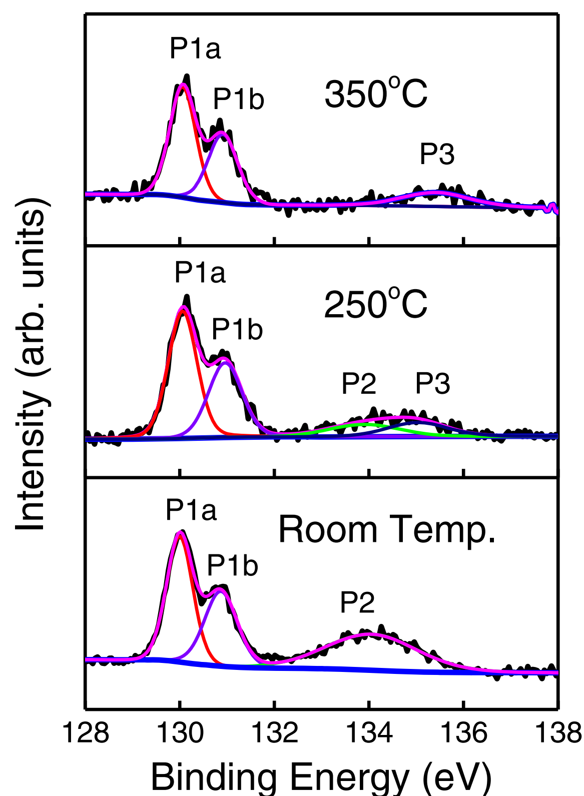

Fig. 5 P 2p XPS spectra of the interface between Al_2O_3 and BP of samples at different deposition temperatures. P1a(P2$p_{3/2}$)and P1b(P 2$p_{1/2}$) represent phosphorus bonded to phosphorus; P2 and P3 represent the different oxidative species of PO_x and P_2O_5, respectively

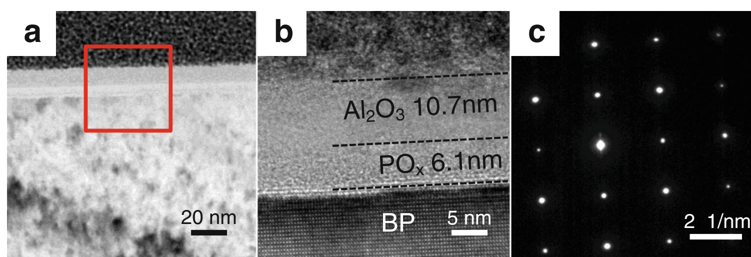

Fig. 6 **a** Low-magnification TEM image of Al_2O_3/BP sample fabricated at 200 °C. **b** High-resolution TEM image of Al_2O_3/BP sample, same scanned region marked by a *red square* in **a**. The thickness of Al_2O_3 and PO_x layer is 10.7 and 6.1 nm, respectively. **c** Selected area electron diffraction (SAED) pattern for the BP crystalline in **b**

the P 2p core level after growth of 100 cycles Al_2O_3 by PEALD at 250 and 350 °C, respectively. The peaks which labeled as P1a and P1b correspond to P-P bonds. The phosphorus core level contains only the characteristic doublet representing the P $2p_{3/2}$ (P1a) and P $2p_{1/2}$ (P1b) orbitals with peak positions of 130.06 eV and 130.92 eV, respectively, consistent with the report [34]. Two peaks of P2 and P3 were observed at 134.07 and 135.03 eV, corresponding to the PO_x and P_2O_5, respectively, as shown in the middle panel. It can be seen that the PO_x peak locates at 134.07 eV, smaller than that of reported P_2O_3 (134.2 eV) [44], which may be caused by less O concentration in the interfacial PO_x layer. The P3 represents the most dominant oxide component and appears at 135.03 eV, in good agreement with the reported P_2O_5 binding energies which are between 135.0 eV [45] and 135.15 eV [37]. When the temperature goes up to 350 °C, interestingly, P2 peak disappears. This is due to the conversion from PO_x to P_2O_5, with the help of reactivity of O_2 plasma at high temperatures. However, there is no P3 peak for natively oxidized BP at room temperature and its peaks of P1a; P1b and P2 locate at 130.06 eV(P $2p_{3/2}$), 130.87 eV(P $2p_{1/2}$), and 134.05 eV, respectively. The absence of P3 peak is due to low temperature or insufficient exposure time for the formation of fully oxidative top layer, which may prevent PO_x from converting into P_2O_5 film.

Finally, the interface properties of Al_2O_3/BP samples were also characterized by TEM measurements. It can be clearly seen for Fig. 6a that the interfacial PO_x layer between Al_2O_3 and BP was formed during PEALD process with the 20 cycles O_2 plasma pretreatment. Figure 6b shows high-resolution TEM (HRTEM) image of the Al_2O_3/BP sample after the deposition of 100 cycles Al_2O_3, same scanned region marked by a red square in Fig. 6a. The thickness of PO_x and Al_2O_3 is 6.1 and 10.7 nm, respectively. It is worth noting that Al_2O_3 and PO_x film is amorphous, while our BP sample is single crystalline which is verified by results of selected area electron diffraction (SAED) pattern, as seen from Fig. 6c. This interfacial layer PO_x was evidenced by TEM results, indicative of O_2 plasma penetrating into PO_x layer and reacting with underlying BP.

Conclusions

In summary, we have demonstrated the direct growth of Al_2O_3 film on BP by using PEALD. The A_{1g} peak of freshly exfoliated BP sample shifts downwards owing to the formation of PO_x in the BP surface. The uniform Al_2O_3 film on BP can be achieved by PEALD with O_2 plasma and TMA precursors, which may be attributed to the etching and reactivity of O_2 plasma with BP at high temperatures. The interfacial layer of PO_x between Al_2O_3 and BP was converted into P_2O_5 as the deposition temperature increases to 350 °C, revealed by XPS characterizations. These findings provide insightful information on passivation and top-gate dielectric integration for future applications in BP devices.

Acknowledgements

This work was supported in part by the start-up program JIH1233003 at Fudan University and also sponsored by Shanghai Pujiang Program (16PJ1400800), China.

Authors' Contributions

BBW and HMZ carried out the BP fabrication and Al_2O_3 growth and measurements. YQD and WJL supervised the work and drafted the manuscript. HLL, PZ, LC, QQS, SJD, and DWZ helped to analyze the experimental results. All authors read and approved the final manuscript.

Competing Interests

The authors declare that they have no competing interests.

Publisher's Note

Springer Nature remains neutral with regard to jurisdictional claims in published maps and institutional affiliations.

Received: 15 December 2016 Accepted: 20 March 2017
Published online: 20 April 2017

References

1. Novoselov KS, Geim AK, Morozov SV, Jiang D, Zhang Y, Dubonos SV et al (2004) Electric field effect in atomically thin carbon films. Science 306:666–669
2. Patil UV, Pawbake AS, Machuno LG, Gelamo RV, Jadkar SR, Late DJ et al (2016) Effect of plasma treatment on multilayer graphene: X-ray photoelectron spectroscopy, surface morphology investigations and work function measurements. RSC Adv 6:48843–48850
3. Radisavljevic B, Radenovic A, Brivio J, Giacometti IV, Kis A (2011) Single-layer MoS_2 transistors. Nat Nanotechnol 6:147–150

4. Late DJ, Liu B, Matte HR, Dravid VP, Rao CNR (2012) Hysteresis in single-layer MoS_2 field effect transistors. ACS Nano 6:5635–5641
5. Liu B, Ma Y, Zhang A, Chen L, Abbas AN, Zhou C et al (2016) High-performance WSe_2 field-effect transistors via controlled formation of in-plane heterojunctions. ACS Nano 10:5153–5160
6. Ovchinnikov D, Allain A, Huang YS, Dumcenco D, Kis A (2014) Electrical transport properties of single-layer WS_2. ACS Nano 8:8174–8181
7. Pradhan NR, Rhodes D, Feng S, Xin Y, Memaran S, Balicas L et al (2014) Field-effect transistors based on few-layered α-$MoTe_2$. ACS Nano 8:5911–5920
8. Late DJ (2016) Temperature-dependent phonon shifts in atomically thin $MoTe_2$ nanosheets. Appl Mater Today 5:98–102
9. Pei T, Bao L, Wang G, Ma R, Yang H, Gao HJ et al (2016) Few-layer $SnSe_2$ transistors with high on/off ratios. Appl Phys Lett 108:053506
10. Erande MB, Suryawanshi SR, More MA, Late DJ (2015) Electrochemically exfoliated black phosphorus nanosheets—prospective field emitters. Eur J Inorg Chem 2015:3102–3107
11. Suryawanshi SR, More MA, Late DJ (2016) Exfoliated 2D black phosphorus nanosheets: field emission studies. J Vac Sci Technol B: Nanotechnol Microelectron: Mater Process Meas Phenom 34:041803
12. Suryawanshi SR, More MA, Late DJ (2016) Laser exfoliation of 2D black phosphorus nanosheets and their application as a field emitter. RSC Adv 6:112103–112108
13. Late DJ (2016) Liquid exfoliation of black phosphorus nanosheets and its application as humidity sensor. Microporous Mesoporous Mater 225:494–503
14. Erande MB, Pawar MS, Late DJ (2016) Humidity sensing and photodetection behavior of electrochemically exfoliated atomically thin-layered black phosphorus nanosheets. ACS Appl Mater Interfaces 8:11548–11556
15. Late DJ (2015) Temperature dependent phonon shifts in few-layer black phosphorus. ACS Appl Mater Interfaces 7:5857–5862
16. Pawbake AS, Erande MB, Jadkar SR, Late DJ (2016) Temperature dependent Raman spectroscopy of electrochemically exfoliated few layer black phosphorus nanosheets. RSC Adv 6:76551–76555
17. Dai J, Zeng XC (2014) Bilayer phosphorene: effect of stacking order on bandgap and its potential applications in thin-film solar cells. J Phys Chem Lett 5:1289–1293
18. Li LK, Yu YJ, Ye GJ, Ge QQ, Chen XH, Zhang YB et al (2014) Black phosphorus field-effect transistors. Nat Nanotechnol 9:372–377
19. Wang QH, Kalantar-Zadeh K, Kis A, Coleman JN, Strano MS (2012) Electronics and optoelectronics of two-dimensional transition metal dichalcogenides. Nat Nanotechnol 7:699–712
20. Xia F, Wang H, Xiao D, Dubey M, Ramasubramaniam A (2014) Two-dimensional material nanophotonic. Nat Photonics 8:899–907
21. Jamieson JC (1963) Crystal structures adopted by black phosphorus at high pressures. Science 139:1291–1292
22. Xia F, Wang H, Jia Y (2014) Rediscovering black phosphorus as an anisotropic layered material for optoelectronics and electronics. Nat Commun 5:4458–4463
23. Liu XK, Ang K-W, Yu WJ, He JZ, Feng XW, Liu Q et al (2016) Black phosphorus based field effect transistors with simultaneously achieved near ideal subthreshold swing and high hole mobility at room temperature. Sci Rep 6:24920
24. Keyes RW (1953) The electrical properties of black phosphorus. Phys Rev 92:580–584
25. Takao Y, Asahina H, Morita AJ (1981) Electronic structure of black phosphorus in tight binding approach. J Phys Soc Jpn 50:3362–3369
26. Liu H, Neal AT, Zhu Z, Xu XF, Tomanek D, Ye PD et al (2014) Phosphorene: an unexplored 2D semiconductor with a high hole mobility. ACS Nano 8:4033–4041
27. Wood JD, Wells SA, Jariwala D, Chen K, Cho E, Sangwan VK et al (2014) Effective passivation of exfoliated black phosphorus transistors against ambient degradation. Nano Lett 14:6964–6970
28. Castellanos-Gomez A, Vicarelli L, Prada E, Island JO, Blanter SI, Buscema M et al (2014) Isolation and characterization of few-layer black phosphorus. 2D Mater 1:025001
29. Li LK, Ye GJ, Tran V, Fei RX, Chen XH, Zhang YB et al (2015) Quantum oscillations in a two-dimensional electron gas in black phosphorus thin films. Nat Nanotechnol 10:608–613
30. Gillgren N, Wickramaratne D, Shi Y, Espiritu T, Yang JW, Hu J et al (2015) Gate tunable quantum oscillations in airstable and high mobility few-layer phosphorene heterostructures. 2D Mater 2:011001
31. Chen XL, Wu YY, Wu ZF, Han Y, Xu SG, Wang L et al (2015) High-quality sandwiched black phosphorus heterostructure and its quantum oscillation. Nat Commun 6:7315
32. Cao Y, Mishchenko A, Yu GL, Khestanova E, Rooney AP, Prestat E et al (2015) Quality heterostructures from two dimensional crystals unstable in air by their assembly in inert atmosphere. Nano Lett 15:4914–4921
33. Avsar A, Vera-Marun IJ, Tan JY, Watanabe K, Taniguchi T, Neto AHC et al (2015) Air-stable transport in graphene-contacted, fully encapsulated ultrathin black phosphorus-based field-effect transistors. ACS Nano 9:4138–4145
34. Edmonds MT, Tadich A, Carvalho A, Ziletti A, Donnell KMO, Koenig SP et al (2015) Creating a stable oxide at the surface of black phosphorus. ACS Appl Mater Interfaces 7:14557–14562
35. Pei JJ, Gai X, Yang J, Wang XB, Choi D-K, Lu YR et al (2016) Producing air-stable monolayers of phosphorene and their defect engineering. Nat Commun 7:10450
36. Zhou QH, Chen Q, Tong YL, Wang JL (2016) Light-induced ambient degradation of Few-layer black phosphorus: mechanism and protection. Angew Chem 128:11609–11613
37. Zhu H, McDonnell S, Qin XY, Azcatl A, Cheng LX, Wallace RM et al (2015) Al_2O_3 on black phosphorus by atomic layer deposition: an in situ interface study. ACS Appl Mater Interfaces 7:13038–13043
38. Liu H, Neal AT, Si M, Du YC, Ye PD (2014) The effect of dielectric capping on few-layer phosphorene transistors: tuning the Schottky barrier heights. IEEE Electron Device Lett 35:795–797
39. Luo X, Rahbarihagh Y, Hwang James CM, Liu H, Du YC, Ye PD (2014) Temporal and thermal stability of Al_2O_3-passivated phosphorene MOSFETs. IEEE Electron Device Lett 35:1314–1316
40. Luo W, Milligan CA, Du Y, Yang L, Wu Y, Ye PD et al (2016) Surface chemistry of black phosphorus under a controlled oxidative environment. Nanotechnology 27:434002
41. Ha SC, Choi E, Kim SH, Roh JS (2005) Influence of oxidant source on the property of atomic layer deposited Al_2O_3 on hydrogen-terminated Si substrate. Thin Solid Films 476:252–257
42. Castellanos-Gomez A, Buscema M, Molenaar R, Singh V, Janssen L, Steele GA et al (2014) Deterministic transfer of two-dimensional materials by all-dry viscoelastic stamping. 2D Mater 1:011002
43. Lu WL, Nan HY, Hong JH, Chen YM, Ni ZH, Jin CH et al (2014) Plasma-assisted fabrication of monolayer phosphorene and its Raman characterization. Nano Res 7:853–859
44. Rokugawa H, Adachi S (2010) Investigation of rapid thermally annealed GaP (001) surfaces in vacuum. Surf Interface Anal 42:88–94
45. Gaskell KJ, Smith MM, Sherwood PMA (2004) Valence band x-ray photoelectron spectroscopic studies of phosphorus oxides and phosphates. J Vac Sci Technol A 22:1331–1336

Submit your manuscript to a SpringerOpen journal and benefit from:

- ► Convenient online submission
- ► Rigorous peer review
- ► Immediate publication on acceptance
- ► Open access: articles freely available online
- ► High visibility within the field
- ► Retaining the copyright to your article

Submit your next manuscript at ► springeropen.com